

Crystal Structures and Thermal Properties of 2,6-Dinitrophenol Complexes with Lanthanide Series

Eun-Ju Kim, Chong-Hyeak Kim,[†] Jae-Kyung Kim,[‡] and Sock-Sung Yun*

Department of Chemistry, Chungnam National University, Daejeon 305-764, Korea. *E-mail: sssyun@cnu.ac.kr

[†]Center for Chemical Analysis, Korea Research Institute of Chemical Technology, P.O. Box 107, Daejeon 305-606, Korea

[‡]High Explosive Team, Agency for Defense Development, P.O. Box 35-5, Daejeon 305-600, Korea

Received March 6, 2008

2,6-Dinitrophenol (2,6-DNP) complexes with lanthanide series including yttrium (except Pm, Tm, and Lu) have been synthesized and their crystal structures have been analyzed by X-ray diffraction methods. Single-crystal X-ray structure determinations have been performed at 296 K on the Ce→Yb species and shown them to be isomorphous, triclinic, $P\bar{1}$, $a = 8.6558(2) \rightarrow 8.5605(3) \text{ \AA}$, $b = 11.8813(3) \rightarrow 11.6611(4) \text{ \AA}$, $c = 13.9650(3) \rightarrow 13.8341(5) \text{ \AA}$, $\alpha = 73.785(1) \rightarrow 73.531(2)^\circ$, $\beta = 74.730(1) \rightarrow 74.903(2)^\circ$, $\gamma = 69.124(1) \rightarrow 69.670(2)^\circ$, $V = 1266.86(5) \rightarrow 1221.53(7) \text{ \AA}^3$, $Z = 2$. In Ln(III) complexes, three 2,6-DNP ligands coordinate directly to the metal ion in the bidentate fashion. The nine coordinated Ln(III) ion forms slightly distorted tri-capped trigonal prism. There are no water molecules in the crystal lattice. The dependences of metal to ligand bond lengths are discussed on the atomic number of lanthanide elements. The thermal properties of lanthanide complexes of 2,6-DNP have also studied by TG-DTG and DSC thermal analysis methods.

Key Words : Lanthanide, 2,6-Dinitrophenol, Crystal structure, Thermal analysis

Introduction

As potential applications of lanthanide complexes have been increased in various fields, the studies to understand the coordination structure and develop novel complexes of lanthanide ions in both solution and solid states have notably revived.¹ The molecular structures of lanthanide complexes of picric acid have been thoroughly studied through the series of lanthanide elements by Horrofield *et al.*² It has been found that the coordination environments around the metal ions for the lanthanide complexes are different between the lighter members and heavier members of lanthanide series. It has been well known that thermodynamic parameters for lanthanide complexation in aqueous solution vary with the cationic radius and the change of the coordination number around the element gadolinium.³

We have reported the crystal structures and thermal properties of some lanthanide complexes of 2,6-DNP and picric acid.⁴ It showed that the coordination behavior of 2,6-DNP is quite different with that of picric acid. Compared to the picric acid, the absence of nitro group at para position on 2,6-DNP makes the nitro group at ortho position of the phenolate be involved strongly in the chelate formation.

As the study to confirm the effect of the cationic radius and the coordination behavior of the nitrophenols in a series of lanthanide complexes of 2,6-DNP in solid state, we have now completed the determination of crystal structures and thermal decomposition parameters for the whole series (except Pm, Tm, and Lu) of lanthanide complexes of 2,6-DNP.

Experimental

Preparation and analysis of the complexes. The prepara-

tion and analysis of the complexes are same as that reported previously.^{4,5} The chemical analysis of the complexes was performed with a CE Instruments EA-1110 elemental analyzer and Jobin-Yvin Ultima-C inductively coupled plasma-atomic emission spectrometer, respectively. The complexes are relatively stable in ambient condition. The results are well agreed with the calculated values. Anal. calcd. (%) for $C_{18}H_{15}N_6O_{18}Ce$: C, 29.08; H, 2.03; N, 11.30; Ce, 18.85. Found: C, 29.21; H, 1.92; N, 11.21; Ce, 18.79. Anal. calcd. (%) for $C_{18}H_{15}N_6O_{18}Pr$: C, 29.05; H, 2.03; N, 11.29; Pr, 18.93. Found: C, 29.61; H, 1.89; N, 11.12; Pr, 18.87. Anal. calcd. (%) for $C_{18}H_{15}N_6O_{18}Sm$: C, 28.68; H, 2.01; N, 11.15; Sm, 19.95. Found: C, 29.22; H, 1.83; N, 11.03; Sm, 19.92. Anal. calcd. (%) for $C_{18}H_{15}N_6O_{18}Eu$: C, 28.62; H, 2.00; N, 11.13; Eu, 20.12. Found: C, 29.60; H, 1.82; N, 10.98; Eu, 20.01. Anal. calcd. (%) for $C_{18}H_{15}N_6O_{18}Gd$: C, 28.42; H, 1.99; N, 11.05; Gd, 20.67. Found: C, 29.24; H, 1.85; N, 10.98; Gd, 20.58. Anal. calcd. (%) for $C_{18}H_{15}N_6O_{18}Dy$: C, 28.23; H, 1.97; N, 10.97; Dy, 21.22. Found: C, 29.30; H, 1.84; N, 10.95; Dy, 21.19. Anal. calcd. (%) for $C_{18}H_{15}N_6O_{18}Ho$: C, 28.14; H, 1.97; N, 10.94; Ho, 21.47. Found: C, 29.09; H, 1.50; N, 10.17; Ho, 21.43. Anal. calcd. (%) for $C_{18}H_{15}N_6O_{18}Er$: C, 28.06; H, 1.96; N, 10.91; Er, 21.70. Found: C, 28.99; H, 1.83; N, 10.90; Er, 21.65. Anal. calcd. (%) for $C_{18}H_{15}N_6O_{18}Yb$: C, 27.85; H, 1.95; N, 10.82; Yb, 22.29. Found: C, 27.72; H, 1.85; N, 10.79; Yb, 22.23.

X-ray crystallography. The epoxy-coated crystal was mounted on a Bruker SMART APEX II X-ray diffractometer equipped with a graphite-monochromated Mo $K\alpha$ radiation ($\lambda = 0.71073 \text{ \AA}$) and a CCD area detector. The intensity data were collected in the phi and omega scan mode with operating 50 kV, 30 mA at 296 K.⁶ The data reduction was performed using the SAINT and SADABS programs.⁷

All calculations in the structural solution and refinement were performed using the Bruker SHELXTL program.⁸ The structure was solved by the heavy atom method and refined by full-matrix least-squares methods. All the non-hydrogen atoms were refined with anisotropically; the hydrogen atoms were geometrically positioned and fixed with the isotropic thermal parameters. The crystallographic data and detailed information of structure solution and refinement are listed in Table 1.

Crystallographic data for the structure reported here have been deposited with the Cambridge Crystallographic Data Centre (Deposition No. are CCDC-680575, 680576, 680577, 680578, 680579, 680580, 680581, 680582, and 680583 for Ce(III), Pr(III), Sm(III), Eu(III), Gd(III), Dy(III), Ho(III), Er(III), and Yb(III) complexes, respectively). The data can be obtained free of charge via www.ccdc.cam.ac.uk/conts/retrieving.html (or from the CCDC, 12 Union Road, Cambridge CB2 1EZ, UK; fax: +44 1223 336033; e-mail: deposit@ccdc.cam.ac.uk).

Thermal analysis. The thermal decomposition of the complex was investigated on a Mettler-Toledo TGA 50 apparatus and Mettler-Toledo DSC model 821^e apparatus. The experimental procedure for the thermal analysis is similar to that described previously.⁵

Results and Discussion

The crystal data for 2,6-DNP complexes of the lanthanide series (except Pm, Tm, and Lu) along with yttrium are given in Table 1. They are all appeared to be triclinic, $P\bar{1}$, similar

unit cells, suggesting an isomorphous iso-structural series, except lanthanum complex which is $Z = 1$ dimeric structure. The variations in unit cell dimensions throughout the series are generally monotonic in consequence of the lanthanide contraction with a decrease in the volume. The lanthanide complexes appeared to be tri-hydrated neutral complexes $[\text{Ln}(2,6\text{-DNP})_3(\text{H}_2\text{O})_3]$ except the lanthanum complex. There are no water molecules in the outer sphere of the complexes. An ORTEP diagram of the molecular structure for the holmium complex as an example is presented by the atom numbering scheme in Figure 1.

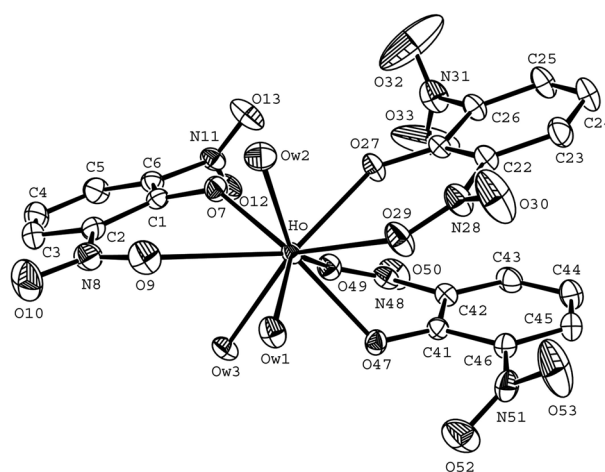


Figure 1. Ortep-3 diagram of $[\text{Ho}(2,6\text{-DNP})_3(\text{H}_2\text{O})_3]$ showing atom labeling. Thermal ellipsoids are drawn at the 30% probability level.

Table 1. Crystal data and structure refinement for $[\text{Ln}(2,6\text{-DNP})_3(\text{H}_2\text{O})_3]$. All crystals are triclinic, space group $P\bar{1}$, $Z = 2$. The stoichiometry is $\text{C}_{18}\text{H}_{15}\text{N}_6\text{O}_{18}\text{Ln}$ (except La: $Z=1$, $[\text{La}_2(2,6\text{-DNP})_6(\text{H}_2\text{O})_4]\cdot 4\text{H}_2\text{O}$, $\text{C}_{36}\text{H}_{34}\text{N}_{12}\text{O}_{38}\text{La}_2$)

Compound	La ^a	Ce	Pr	Nd ^a	Sm	Eu
Formula weight	1520.57	743.48	744.27	747.60	753.71	755.32
Unit cell dimensions						
<i>a</i> (Å)	9.162(1)	8.6558(2)	8.6468(1)	8.6451(5)	8.626(1)	8.620(1)
<i>b</i> (Å)	12.252(6)	11.8813(3)	11.8569(2)	11.8493(7)	11.806(1)	11.782(1)
<i>c</i> (Å)	12.570(1)	13.9650(3)	13.9296(2)	13.923(1)	13.8704(2)	13.8619(2)
α (°)	107.60(2)	73.785(1)	73.828(1)	73.800(5)	73.784(1)	73.786(1)
β (°)	100.74(1)	74.730(1)	74.729(1)	74.710(5)	74.653(1)	74.680(1)
γ (°)	96.98(2)	69.124(1)	69.191(1)	69.236(5)	69.301(1)	69.365(1)
Volume (Å ³)	1297.5(7)	1266.86(5)	1260.45(3)	1258.9(1)	1246.85(3)	1243.36(3)
Calculated density (g/cm ³)	1.946	1.949	1.961	1.972	2.008	2.017
Absorption coefficient (mm ⁻¹)	1.750	1.897	2.034	2.164	2.457	2.625
F(000)	752	734	736	738	742	744
θ range for data collection (°)	2.04-24.97	1.54-28.34	1.55-28.26	1.88-27.50	1.56-28.34	1.56-28.27
Index ranges	-10 ≤ <i>h</i> ≤ 10	-9 ≤ <i>h</i> ≤ 11	-11 ≤ <i>h</i> ≤ 11	-1 ≤ <i>h</i> ≤ 11	-11 ≤ <i>h</i> ≤ 11	-11 ≤ <i>h</i> ≤ 11
	-14 ≤ <i>k</i> ≤ 13	-15 ≤ <i>k</i> ≤ 15	-15 ≤ <i>k</i> ≤ 15	-14 ≤ <i>k</i> ≤ 15	-15 ≤ <i>k</i> ≤ 15	-15 ≤ <i>k</i> ≤ 14
	0 ≤ <i>l</i> ≤ 14	-18 ≤ <i>l</i> ≤ 18	-18 ≤ <i>l</i> ≤ 18	-17 ≤ <i>l</i> ≤ 18	-18 ≤ <i>l</i> ≤ 18	-18 ≤ <i>l</i> ≤ 18
Reflections collected/unique	4739/4516	24836/6262	24451/6114	6904/5757	24184/6164	24229/6042
	[R(int)=0.0271]	[R(int)=0.0192]	[R(int)=0.0157]	[R(int)=0.0558]	[R(int)=0.0196]	[R(int)=0.0173]
Data/restraints/parameters	4516/0/407	6262/0/424	6114/0/412	5757/0/412	6164/0/412	6042/0/413
Goodness-of-fit on F^2	1.057	1.071	1.071	1.051	1.037	1.061
Final R indices	R ₁ =0.0283,	R ₁ =0.0248,	R ₁ =0.0229,	R ₁ =0.0358,	R ₁ =0.0231,	R ₁ =0.0201,
[<i>I</i> > 2σ(<i>I</i>)]	wR ₂ =0.0741	wR ₂ =0.0657	wR ₂ =0.0612	wR ₂ =0.0734	wR ₂ =0.0575	wR ₂ =0.0511

Table 1. Continued

Compound	Gd	Tb ^a	Dy	Ho	Er	Yb	Y ^a
Formula weight	760.61	762.28	765.86	768.29	770.62	776.40	692.27
Unit cell dimensions							
<i>a</i> (Å)	8.6107(1)	8.5916(8)	8.5950(2)	8.584(1)	8.574(1)	8.5605(3)	8.5876(6)
<i>b</i> (Å)	11.7601(2)	11.734(2)	11.7243(2)	11.7057(2)	11.686(1)	11.6611(4)	11.7161(9)
<i>c</i> (Å)	13.8551(2)	13.809(2)	13.8373(3)	13.8335(2)	13.8265(2)	13.8341(5)	13.862(1)
α (°)	73.741(1)	73.79(2)	73.711(1)	73.641(1)	73.620(1)	73.531(2)	73.531(7)
β (°)	74.707(1)	74.66(1)	74.689(1)	74.757(1)	74.815(1)	74.903(2)	74.745(6)
γ (°)	69.407(1)	69.44(2)	69.499(1)	69.573(1)	69.651(1)	69.670(2)	69.590(6)
Volume (Å ³)	1239.32(3)	1230.0(3)	1232.14(4)	1228.71(3)	1225.36(3)	1221.53(7)	1232.4(2)
Calculated density (g/cm ³)	2.038	2.058	2.064	2.077	2.089	2.111	1.865
Absorption coefficient (mm ⁻¹)	2.779	2.979	3.136	3.324	3.529	3.933	2.470
F(000)	746	748	750	752	754	758	696
θ range for data collection (°)	1.56-28.48	2.19-24.97	1.56-28.32	1.56-28.30	1.56-28.32	1.56-28.35	1.90-27.50
Index ranges	-11 ≤ <i>h</i> ≤ 10 -15 ≤ <i>k</i> ≤ 15 -17 ≤ <i>l</i> ≤ 18	-9 ≤ <i>h</i> ≤ 10 -13 ≤ <i>k</i> ≤ 13 0 ≤ <i>l</i> ≤ 16	-11 ≤ <i>h</i> ≤ 11 -15 ≤ <i>k</i> ≤ 15 -18 ≤ <i>l</i> ≤ 18	-11 ≤ <i>h</i> ≤ 11 -15 ≤ <i>k</i> ≤ 15 -18 ≤ <i>l</i> ≤ 18	-11 ≤ <i>h</i> ≤ 11 -15 ≤ <i>k</i> ≤ 15 -18 ≤ <i>l</i> ≤ 17	-11 ≤ <i>h</i> ≤ 11 -15 ≤ <i>k</i> ≤ 15 -18 ≤ <i>l</i> ≤ 18	-1 ≤ <i>h</i> ≤ 11 -14 ≤ <i>k</i> ≤ 14 -17 ≤ <i>l</i> ≤ 18
Reflections collected/unique	24198/6162 [R(int)=0.0169]	4502/4308 [R(int)=0.0558]	24201/6111 [R(int)=0.0182]	24021/6091 [R(int)=0.0153]	23879/6079 [R(int)=0.0177]	24269/6065 [R(int)=0.0177]	6755/5632 [R(int)=0.0355]
Data/restraints/parameters	6162/0/412	4308/0/379	6111/0/412	6091/0/412	6079/0/412	6065/0/412	5632/0/414
Goodness-of-fit on <i>F</i> ²	1.082	1.028	1.063	1.063	1.088	1.072	1.008
Final R indices [<i>I</i> > 2σ(<i>I</i>)]	R ₁ =0.0194, wR ₂ =0.0504	R ₁ =0.0523, wR ₂ =0.1513	R ₁ =0.0186, wR ₂ =0.0473	R ₁ =0.0174, wR ₂ =0.0444	R ₁ =0.0180, wR ₂ =0.0472	R ₁ =0.0170, wR ₂ =0.0426	R ₁ =0.0576, wR ₂ =0.1011

^aref. [4].

The crystal structure of lanthanum complex of 2,6-DNP has shown to be a unique octa-hydrated dinuclear complex whose stoichiometric chemical formula is [La₂(2,6-DNP)₆(H₂O)₄·4H₂O]^{4c}. As we discussed previously for 2,6-DNP complexes of Nd(III), Tb(III), and Y(III) ions,⁴ the structural feature of complexes is the presence of three 2,6-DNP ligands coordinated in bidentate fashion directly to the metal ion also for the rest of lanthanide ions. The skeletal structure around the Ln(III) ion forms a slightly distorted tri-capped trigonal prism. The oxygen atoms of nitro groups, O_n (9,29,49) lie close enough to the metal atom to be considered to have a significant bidentate interaction. Therefore, Ln(III) ion forms three six-membered chelate rings with each 2,6-DNP through an O_n(9,29,49) atom of the nitro group and an O_p(7,27,47) atom of the phenolate group; in the chelate rings, O_p(7,27,47)-Ln-O_n(9,29,49) lie around 65°. Figure 2 shows the coordination polyhedron of the Ho(III) ion of the complex as an example.

The selected bond lengths and angles for the complexes are listed in Table 2. As "so called" the lanthanide contraction, the cationic radii decreases linearly with the increase of atomic number through lanthanide series.⁹ Since the metal to ligand bonds in lanthanide complexes are predominantly electrostatic, the linear relationship must be reflected on the bond lengths between metal and ligand of lanthanide complexes. The trends of the variations of the bond lengths for the coordinated water molecules, Ln-O_w(1,2,3) and for the coordinated phenolates, Ln-O_p(7,27,47) are consistent with the lanthanide contraction. The bond distances between metal and oxygen atoms are very close each other in a given metal for coordinated water molecules and phenolates. For

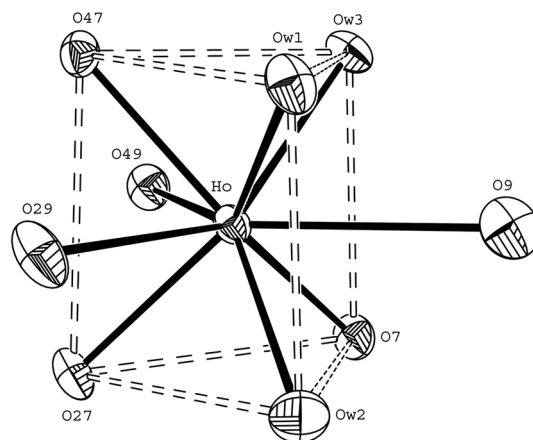


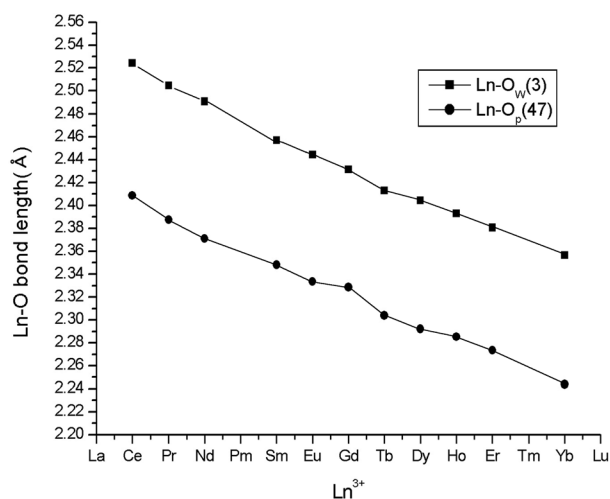
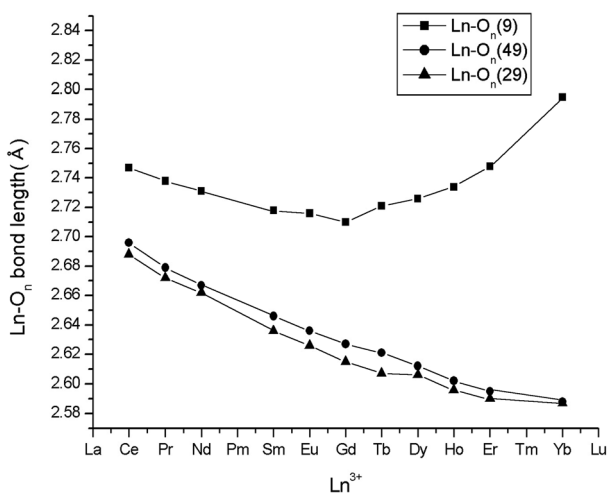
Figure 2. The coordination polyhedron of the Ho(III) ion in [Ho(2,6-DNP)₃(H₂O)₃]. The tricapped trigonal prism is indicated by dashed lines.

the coordinated water molecules, Ln-O_w(1,2,3) all contract noticeably and uniformly in the range of 2.473(1)-2.287(2) Å for Ln-O_w(1), 2.498(2)-2.333(2) Å for Ln-O_w(2), and 2.524(1)-2.356(2) Å for Ln-O_w(3). For the coordinated phenolate groups, Ln-O_p(7,27,47) all contract fairly uniformly in the range of 2.346(1)-2.183(2) Å for Ln-O_p(7), 2.371(1)-2.222(2) Å for Ln-O_p(27), and 2.409(1)-2.244(2) Å for Ln-O_p(47). Figure 3 shows fairly the linear variations of the bond lengths for the coordinated water oxygen and phenolate oxygen across the lanthanide series, reflecting that metal to ligand bonds are predominantly electrostatic for the coordinated water and phenolate.

Of particular interest with the coordination sphere of the metal atom is the role of the ortho-nitro groups of the

Table 2. Selected bond lengths (Å) and angles (°) for complexes

Atoms	Ce	Pr	Nd ^a	Sm	Eu	Gd	Tb ^a	Dy	Ho	Er	Yb
Ln-O _p (7)	2.346(1)	2.327(2)	2.312(3)	2.284(2)	2.273(2)	2.265(2)	2.247(5)	2.234(2)	2.221(2)	2.208(2)	2.183(2)
Ln-O _p (27)	2.371(1)	2.355(2)	2.343(3)	2.311(2)	2.300(2)	2.292(2)	2.279(5)	2.263(2)	2.250(2)	2.239(2)	2.222(2)
Ln-O _p (47)	2.409(1)	2.388(2)	2.371(3)	2.348(2)	2.334(2)	2.329(2)	2.304(5)	2.292(2)	2.285(2)	2.274(2)	2.244(2)
Ln-O _w (1)	2.473(1)	2.453(2)	2.435(3)	2.399(2)	2.384(2)	2.370(2)	2.346(5)	2.339(2)	2.326(2)	2.309(2)	2.287(2)
Ln-O _w (2)	2.498(2)	2.483(2)	2.469(3)	2.436(2)	2.421(2)	2.409(2)	2.401(7)	2.379(2)	2.368(2)	2.354(2)	2.333(2)
Ln-O _w (3)	2.524(1)	2.505(2)	2.491(3)	2.457(2)	2.445(2)	2.431(2)	2.413(6)	2.404(2)	2.393(2)	2.381(2)	2.356(2)
Ln-O _n (29)	2.688(1)	2.672(2)	2.662(3)	2.636(2)	2.626(2)	2.615(2)	2.607(6)	2.606(2)	2.596(2)	2.590(2)	2.587(2)
Ln-O _n (49)	2.696(1)	2.679(2)	2.667(4)	2.646(2)	2.636(2)	2.627(2)	2.621(6)	2.612(2)	2.602(2)	2.595(2)	2.588(2)
Ln-O _n (9)	2.747(2)	2.738(2)	2.731(4)	2.718(2)	2.716(2)	2.710(2)	2.721(7)	2.726(2)	2.734(2)	2.748(2)	2.795(2)
O(7)-Ln-O(9)	62.20(5)	62.52(6)	62.9(1)	63.34(6)	63.48(6)	63.54(6)	63.8(2)	63.50(6)	63.50(6)	63.31(6)	62.67(6)
O(27)-Ln-O(29)	63.51(4)	64.04(6)	64.6(1)	65.12(6)	65.46(6)	65.77(5)	66.2(2)	66.24(6)	66.48(5)	66.75(6)	67.11(6)
O(47)-Ln-O(49)	63.09(4)	63.46(6)	63.7(1)	64.21(6)	64.42(6)	64.64(5)	64.9(2)	65.18(5)	65.31(5)	65.44(5)	65.94(5)
C(1)-O(7)-Ln	136.9(1)	136.7(2)	136.8(3)	136.6(2)	136.5(2)	136.5(1)	136.9(5)	137.1(1)	137.6(1)	137.8(1)	139.2(1)
N(8)-O(9)-Ln	135.3(1)	135.1(2)	134.4(3)	134.3(2)	134.2(2)	134.2(2)	133.0(5)	133.4(2)	133.0(2)	132.7(2)	131.9(2)

^aref. [4].**Figure 3.** The variations of Ln-O bond lengths across the lanthanide series.**Figure 4.** The variations of Ln-O_n bond lengths across the lanthanide series.

coordinated 2,6-DNP ligands. The Ln-O_n(29,49) distances for the coordinated nitro groups decrease fairly linearly in the range of 2.688(1)-2.587(2) Å for Ln-O_n(29) and 2.696

Table 3. The enthalpy of dehydration and explosive decomposition of the complexes [Ln(2,6-DNP)₃(H₂O)₃]

Ln(III)	Dehydration		Decomposition	
	Temp. (°C)	ΔH _{dehy} (kJ/mol)	Temp. (°C)	ΔH _{decom} (kJ/mol)
Ce	126.8	81	302.3	-522
Pr	147.5	38	316.8	-302
Sm	156.3	93	325.8	-1169
Eu	142.6	109	328.7	-1250
Gd	141.0	124	344.7	-1627
Dy	150.5	76	338.2	-741
Ho	149.1	77	341.8	-913
Er	145.8	86	342.8	-956
Yb	151.7	111	345.3	-950

(1)-2.588(2) Å for Ln-O_n(49). However, for the third coordinated nitro group, the Ln-O_n(9) distances decrease in lighter lanthanide family (from 2.747(2) Å of Ce-O_n(9) to 2.710(2) Å of Gd-O_n(9)) and then increase in heavier lanthanide family (from 2.710(2) Å of Gd-O_n(9) to 2.795(2) Å of Yb-O_n(9)). Figure 4 shows the plots of Ln-O_n bond lengths against atomic numbers of lanthanide elements. One of the three nitro groups bonds rather weakly to the metal ion (Ln-O_n(9)). Ln-O_n(9) are ca 0.01-0.20 Å longer than Ln-O_n(29) or Ln-O_n(49). So called “Gadolinium break”, which reflects the tendency to change the coordination number from nine to eight, is clearly appeared in one of the plots (square dot). However, strong ability of 2,6-DNP to make the chelate with the metal ions leaves the coordination number unchanged in the lanthanide series, unlikely with the picrate complexes.

Thermal analysis data (TG-DTG and DSC) for the 2,6-DNP complexes of La(III), Nd(III), and Tb(III) ions had been obtained and discussed previously.^{4c} We now completed the thermal study for the rest of the 2,6-DNP complexes of lanthanide series (except Pm, Tm, and Lu). It is appeared the thermal decomposition mechanism for the complexes are all same as that suggested previously.^{4c} It was suggested that the thermal decomposition reaction of the complexes occurs through three stages under the experimental conditions,

which are the dehydration, the decomposition of metal complex with the explosion of 2,6-DNP, and the formation of the metal oxide.

The dehydration and explosive decomposition energies of the complexes were calculated from DSC data. Table 3 lists the dehydration and explosive decomposition energies of the complexes along with the maximum peak temperatures. It is again found that there are the "Gadolinium break" both in the dehydration and decomposition energies.

We have reached following conclusions. The coordination number of the complexes are unlikely constant as nine across the series. The bond lengths between the cations and oxygen atoms of the coordinated water molecules and phenolate groups varies linearly across the lanthanide series with one exception, reflecting "so called" the lanthanide contraction. However, the dependency of the bond length of the weakest bond between the cation and nitro groups on the atomic numbers of the series are broken at Gadolinium as known so called "Gadolinium break", which is generally appeared in thermodynamic parameters of the lanthanide complexation. "Gadolinium break" is also observed in the dehydration and decomposition energies of the 2,6-DNP complexes of lanthanide series.

References

- (a) Zheng, X.-J.; Jin, L.-P.; Gao, S. *Inorg. Chem.* **2004**, *43*, 1600.
(b) Zhao, B.; Chen, X.-Y.; Cheng, P.; Liao, D.-Z.; Yan, S.-P.; Jiang, Z.-H. *J. Am. Chem. Soc.* **2004**, *126*, 15394. (c) Huh, H. S.; Lee, S. W. *Bull. Korean Chem. Soc.* **2002**, *23*, 948. (d) Huh, H. S.; Lee, S. W. *Bull. Korean Chem. Soc.* **2006**, *27*, 1839. (e) Kremer, C.; Torres, J.; Dominguez, S.; Mederos, A. *Coord. Chem. Rev.* **2005**, *249*, 567. (f) Yun, S.-S.; Oh, Y.; Kang, Me-A.; Kim, Y.-I. *Bull. Korean Chem. Soc.* **2006**, *27*, 309.
- (a) Harrowfield, J. M.; Weimin, L.; Skelton, B. W.; White, A. H. *Aust. J. Chem.* **1994**, *47*, 321. (b) Harrowfield, J. M.; Weimin, L.; Skelton, B. W.; White, A. H. *Aust. J. Chem.* **1994**, *47*, 339. (c) Harrowfield, J. M.; Weimin, L.; Skelton, B. W.; White, A. H. *Aust. J. Chem.* **1994**, *47*, 349. (d) Harrowfield, J. M.; Skelton, B. W.; White, A. H. *Aust. J. Chem.* **1994**, *47*, 359.
- (a) Choppin, G. R. *Pure Apply. Chem.* **1971**, *27*, 23. (b) Choppin, G. R. *J. Less-common Met.* **1985**, *112*, 193.
- (a) Suh, H. R.; Suh, H. S.; Yun, S. S.; Lee, E. K.; Kang, S. K. *Acta Cryst.* **2002**, *C58*, m202. (b) Suh, H. R.; Suh, H. S.; Yun, S. S.; Lee, E. K.; Kang, S. K. *Acta Cryst.* **2002**, *E58*, m284. (c) Yun, S. S.; Suh, H. R.; Suh, H. S.; Kang, S. K.; Kim, J. K.; Kim, C. H. *J. Alloys Comp.* **2006**, *408-412*, 1030.
- Yun, S. S.; Kang, S. K.; Suh, H. R.; Suh, H. S.; Lee, E. K.; Kim, J. K.; Kim, C. H. *Bull. Korean Chem. Soc.* **2005**, *26*, 1197.
- Bruker, *SMART* (Version 5.625) *Data Collection Program*; Bruker AXS Inc.: Madison, Wisconsin, USA, 2001.
- Bruker, *SAINT* (Version 6.28a) and *SADABS* (Version 2.03) *Data Reduction and Absorption Correction Program*; Bruker AXS Inc.: Madison, Wisconsin, USA, 2001.
- Sheldrick, G. M. *SHELXTL* (Version 6.12) *Structure Analysis Program*; Bruker AXS Inc.: Madison, Wisconsin, USA, 2001.
- Greenwood, N. N.; Earnshaw, A. *Chemistry of the Elements*, 2nd ed.; Butterworth-Heinemann: Oxford, 1997; Chapter 30.